Cell, Vol. 87, 1059–1068, December 13, 1996, Copyright ©1996 by Cell Press

# A Drosophila Neurexin Is Required for Septate Junction and Blood-Nerve Barrier Formation and Function

**Stefan Baumgartner,*‖ J. Troy Littleton,†‖ Kendal Broadie,‡# Manzoor A. Bhat†, Ruth Harbecke,§ Judith A. Lengyel,§ Ruth Chiquet-Ehrismann,* Andreas Prokop,‡ and Hugo J. Bellen†**
*Friedrich Miescher-Institute
Postfach 2543
CH-4002 Basel
Switzerland
†Howard Hughes Medical Institute
Department of Molecular and Human Genetics
Baylor College of Medicine
Houston, Texas 77030
‡Department of Zoology
University of Cambridge
Downing Street
Cambridge, CB2 3EJ
United Kingdom
§Department of Molecular, Cell, and Developmental Biology
University of California
Los Angeles, California 90095

## Summary

**Septate and tight junctions are thought to seal neighboring cells together and to function as barriers between epithelial cells. We have characterized a novel member of the neurexin family, Neurexin IV (NRX), which is localized to septate junctions (SJs) of epithelial and glial cells. NRX is a transmembrane protein with a cytoplasmic domain homologous to glycophorin C, a protein required for anchoring protein 4.1 in the red blood cell. Absence of NRX results in mislocalization of Coracle, a Drosophila protein 4.1 homolog, at SJs and causes dorsal closure defects similar to those observed in *coracle* mutants. *nrx* mutant embryos are paralyzed, and electrophysiological studies indicate that the lack of NRX in glial–glial SJs causes a breakdown of the blood-brain barrier. Electron microscopy demonstrates that *nrx* mutants lack the ladder-like intercellular septa characteristic of pleated SJs (pSJs). These studies identify NRX as the first transmembrane protein of SJ and demonstrate a requirement for NRX in the formation of septate-junction septa and intercellular barriers.**

## Introduction

Cell–cell adhesion and communication are essential for multicellular development and function. Specialized junctions have been visualized and classified at the ultrastructural level in most cell types. These junctions are divided into those that mediate cell communication (gap junctions and chemical synapses); those that anchor cells to the extracellular matrix or adjacent cells (adherens junctions, focal contacts, and desmosomes); and those that function as selective-permeability barriers, separating apical and basal boundaries (tight junctions and septate junctions [SJs]) (Bock and Clark, 1987). To understand the function of these junctions further, a definition of the molecular components and their putative roles is imperative. The distribution and type of cell junctions in Drosophila comprise cell–cell, cell–substrate, adherens, gap, and SJs (Lane and Skaer, 1980; Tepass and Hartenstein, 1994). SJs have been described throughout invertebrate phyla and show a characteristic intercellular ladder-like structure in electron micrographs (Lane and Skaer, 1980). As in other insects, SJs in Drosophila are common to all epithelia and can be subdivided into two types: smooth SJs (sSJs; in gut endoderm and Malpighian tubules) and pleated SJs (pSJs; in ectodermally derived epithelia, i.e., glial sheaths, epidermis, trachea, salivary glands, ectodermal parts of the alimentary canal, and imaginal discs) (Lane and Skaer, 1980; Fristrom, 1982; Tepass and Hartenstein, 1994).

Two proteins have been shown to be associated with SJs in Drosophila: Band 4.1-Coracle (Fehon et al., 1994) and Discs-large (DLG; Woods and Bryant, 1991). The Drosophila 4.1-Coracle protein, a homolog of vertebrate protein 4.1, is specifically localized to a subpopulation of pSJs (Fehon et al., 1994). Protein 4.1 in vertebrates is thought to attach the cell cytoskeleton to transmembrane proteins, such as glycophorin C, and to localize signaling proteins (e.g., p55) to specific subcellular contact sites (review Lux and Palek, 1995). The product of the *discs-large* (*dlg*) gene contains PDZ-domains, an SH3 domain, and a domain with homology to guanylate kinases, suggesting a role in cell signaling (Woods and Bryant, 1991). Homologous proteins in vertebrates include the tight junction–associated proteins ZO1 and ZO2 (Itoh et al., 1993; Willott et al., 1993; Jesaitis and Goodenough, 1994). Mutations in Band 4.1-Coracle are embryonic lethal and exhibit cell migration defects during dorsal closure (Fehon et al., 1994), whereas mutations in *dlg* cause a breakdown of SJs in imaginal cells, with a loss of apicobasal cell-polarity and overgrowth (Woods and Bryant, 1991) and defects in synapse formation (Lahey et al., 1994). Hence, based on genetic and morphological studies (Lane and Skaer, 1980; Lane, 1991), SJs have been proposed to play a role in the formation of barriers to prevent paracellular flow between epithelial cells, in cell adhesion, and in inter- and intracellular communication. It has also been suggested that SJs may be the insect equivalent of tight junctions in vertebrates (Willott et al., 1993; Kirkpatrick and Peifer, 1995).

We have identified and characterized a new integral protein of SJs, Neurexin IV (NRX), the first member of the *neurexin* gene family isolated in a nonmammalian species. Neurexins were first identified as synapse-specific extracellular receptors for latrotoxin, a component of black widow spider venom that triggers massive exocytosis (Petrenko et al., 1991). Three *neurexin* genes, described in vertebrates, have large extracellular do-

‖These authors contributed equally to this work.
#Present address: Department of Biology, University of Utah, Salt Lake City, Utah 84112.

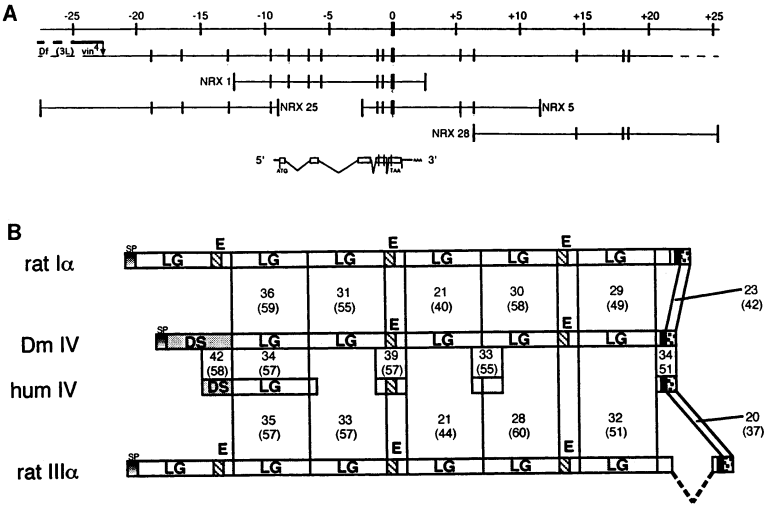


Figure 1. Cloning and Structure of *nrx*

(A) Approximately 50 kb of cloned DNA from the *nrx* chromosomal region defined by four genomic phages are presented with the EcoRI restriction sites. The EcoRI site common to cDNA and genomic DNA is chosen as 0. The proximal molecular break point of *Df(3L)vin*$^4$ is indicated by an arrow. Southern analysis and genomic sequencing data indicate that *nrx* harbors at least four exons.

(B) Schematic drawing of the domain structures and comparison of identities between Drosophila NRX, human Neurexin IV, and rat Neurexin Ia and IIIa. Only partial sequences from human Neurexin IV were available and were drawn where they align to NRX. The top row of numbers indicates percentages of identity, and the bottom row indicates percentages of similarity. Note that in NRX and human Neurexin IV, one laminin G domain (LG) and one EGF-like motif (E) are replaced by a DS domain.

mains with laminin G motifs and epidermal growth factor (EGF) repeats and are expressed exclusively in the brain (Ushkaryov et al., 1992; Ushkaryov and Südhof, 1993). Based on their structure and the finding that rat brain contains more than 1000 neurexin isoforms generated by alternative splicing (Ullrich et al., 1995), it has been proposed that neurexins could serve as cell surface receptors for synaptic targeting in specific subsets of neurons.

Interestingly, the role of neurexins may not be confined to the nervous system. Recently, an intracellular ligand of neurexins, the CASK protein, was identified. CASK is expressed in neuronal and nonneuronal tissues (Hata et al., 1996). This protein shares extensive homology with the SJ-associated protein DLG, the tight junction–associated proteins ZO1 and ZO2, and the postsynaptic density protein PSD95/SAP90 (Woods and Bryant, 1991; Cho et al., 1992; Itoh et al., 1993; Tsukita et al., 1993; Willott et al., 1993; Woods and Bryant, 1993a; Jesaitis and Goodenough, 1994). Taken together, these data suggest that the vertebrate neurexin family likely includes additional members that may participate in a variety of cell-junctional complexes, including tight junctions and synapses.

To dissect the role of neurexins in vivo, we have initiated a mutational analysis of NRX in Drosophila. NRX is localized to pSJs of ectodermally derived epithelial and glial cells and is a novel specific marker for these junctions. Through mutational analysis, electrophysiology, and morphological studies, we demonstrate that NRX plays an essential role in SJ formation and function in glia and epithelial cells. This study defines SJs as essential cellular components required for embryonic development and blood-brain barrier formation and provides novel in vivo insights into the broad role that the neurexin family may play in the function of cellular junctions.

## Results

### Cloning and Sequence of a Novel Drosophila *neurexin*

Degenerate primers complementary to sequences of an EGF domain were used in polymerase chain reactions of Drosophila cDNA libraries and allowed isolation of cDNAs that showed homology to vertebrate neurexins (Brown and Kafatos, 1988). The longest clone, a 5 kb cDNA (cnrx 9), was mapped to 68F. In addition, genomic phage clones were isolated, permitting cloning and restriction mapping of more than 50 kb of genomic DNA (Figure 1A). Structural analyses revealed that the transcription unit spans 12 kb of genomic DNA and contains at least 4 introns (Figure 1A).

The predicted translation product is a protein of 1283 amino acids (145 kDa) (Figure 1B). The initiation methionine is followed by a secretory signal sequence. The primary structure of the protein also contains a domain characteristic of a transmembrane-spanning segment close to the C-terminus, suggesting that the protein is a transmembrane protein with a large extracellular domain. As shown in Figure 1B, the protein shows a domain structure like that of the vertebrate neurexins. The only major difference is in the amino-terminal domain, where a laminin domain and an EGF-like repeat are replaced by a recently identified discoidin (DS) domain, thought to represent a lectin-binding domain. The similarity to neurexins is highest in the EGF modules and lower in the laminin G domains. In addition, the intracellular domain of NRX displays 68% similarity with the intracellular domain of glycophorin C.

A database search using the Drosophila *nrx* cDNA sequence showed a significant homology to human cDNA sequences at 17q21 (Brody et al., 1995; Friedman et al., 1995). The domain structure of the human gene from 17q21 appears more similar than rat neurexins to Drosophila *nrx* and contains an N-terminal DS domain (Figure 1B). The human *neurexin* is expressed in brain, kidney, and lung (Figure 2C). These data suggest that this gene is a human homolog of the fly *nrx* and indicate the existence of a fourth neurexin in vertebrates whose expression is not limited to the nervous system. Therefore, we have named the human homolog *neurexin IV* and the fly homolog *nrx IV*, here abbreviated *nrx*.

Since reports have demonstrated extensive alternative splicing of neurexins in vertebrates, we tested whether alternative splicing occurs within the *nrx* transcription unit. Developmental Northern blot analysis

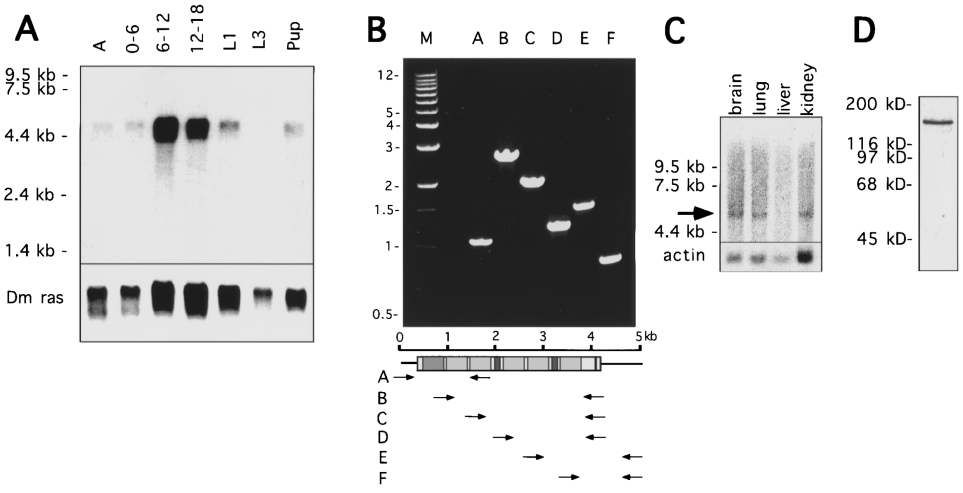


Figure 2. Northern and Western Analyses

(A) Northern-blot analysis of different stages of the Drosophila life cycle with an *nrx* cDNA. Each lane contains 5 mg of poly $A^+$ RNA (hours after egg lay, L1 and L3 are first- and third-instar larva, Pup = pupal stages, A = adults). A 5 kb transcript was identified. The Dm ras 64 probe was used as a loading control. Transcript lengths were determined with RNA standards.

(B) The *nrx* gene does not undergo extensive alternative splicing. RT-polymerase chain reactions using different primer combinations covering almost the whole transcript. In each case, a single band was observed.

(C) Human Northern blot of various embryonic tissues using human *neurexin IV* cDNAs. A single 6 kb transcript is detected in brain, kidney, and lung.

(D) Western analysis of NRX protein of 7–22 hr old embryos. One prominent band of 150–155 kDa was observed, consistent with the predicted molecular weight of the protein.

with *nrx* cDNA probes indicates that the gene is transcribed only zygotically, with its peak of expression between 6 and 18 hr after egg lay (Figure 2A). Therefore, we reverse transcribed mRNA by polymerase chain reactions, applying a comprehensive set of primers. In all cases, only a single band of the expected length was amplified (Figure 2B), suggesting that extensive alternative splicing does not occur in Drosophila *nrx*.

A polyclonal antiserum was raised against a C-terminal peptide. Western analyses show a single band of 150–155 kDa, in close agreement with the predicted size of 145 kDa (Figure 2D). This serum is specific to NRX, as no protein can be detected in Western blots of embryos that carry a deficiency removing the *nrx* gene (*Df(3L)BK9/Df(3L)vin*$^{8}$) or other *nrx* mutations (see below).

### NRX is Localized to pSJs

We analyzed the expression pattern of the *nrx* gene using whole-mount in situ hybridization and antibody stainings. With both methods, the *nrx* gene product can first be detected at late stage 11/early stage 12. NRX is localized to epithelial cells of ectodermal origin such as epidermis, the tracheal system, pharynx, esophagus, proventriculus, hindgut, salivary glands, and cells of the peripheral and central nervous system (P-CNS) (Figure 3). Staining in the PNS is localized to the scolopales of the lateral chordotonal organs (Figures 3D and 5B) and is restricted to glial cells. Double-labeling experiments show that *nrx*-expressing cells in the CNS and along the peripheral nerves express glial-specific cell markers but not neuronal markers. Two types of epithelia do not express NRX: amnioserosa and Malpighian tubules. Interestingly, all tissues that express NRX in the embryo are characterized by the presence of pSJs, with NRX expression first detectable approximately 1 hr prior to their formation (Tepass and Hartenstein, 1994).

To determine in which compartment NRX is localized, we carried out double-labeling experiments. In epidermis and hindgut, NRX is localized apicolaterally, adjacent to Crumbs, which delimits the zonula adherens (Grawe et al., 1996). These two proteins are not coexpressed (Figure 3E), placing NRX apicolaterally. Double labeling of salivary glands with anti-FAS (Woods and Bryant, 1993b) and anti-NRX shows that both proteins colocalize at salivary SJs (data not shown). Double labeling with anti-NRX and anti-D4.1/Coracle antisera demonstrates that NRX precisely colocalizes with this SJ-restricted protein in all tissues tested except PNS and CNS, where D4.1-Coracle is only expressed in a few cells. This colocalization was confirmed in a series of optical sections throughout the embryo using confocal microscopy. In the chordotonal organs, NRX is expressed in the cells surrounding the scolopales where SJs have been localized (S. D. Carlson et al., submitted). In addition, NRX is distributed in a ring at the apical end of many cell types, as shown for SJs (Lane and Skaer, 1980). Postembryonically, in third-instar larvae, staining can also be detected in areas where SJs have been reported: the subperineural sheath of the larval CNS (Lane et al., 1977), imaginal disc cells (Locke, 1965), and salivary glands (data not shown). Thus, NRX is localized to all pSJs documented.

As SJs represent sites of intercellular contact, NRX might function as a cell adhesion molecule. Adhesion properties of proteins can be tested in cell culture using S2 cell adhesion assays (Bieber, 1994). Western blot analysis of uninduced Drosophila S2 cell lines that do not show cell aggregation demonstrated that NRX is normally expressed in these cells. Therefore, NRX is not

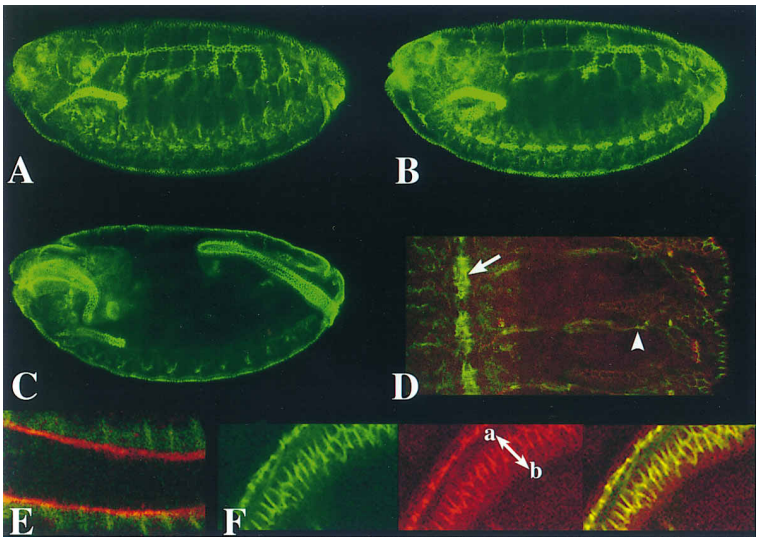


Figure 3. NRX is Expressed in Ectodermally Derived Epithelia and Localized to SJs

Embryos are oriented anteriorly to the left and dorsal side up unless otherwise noted. Confocal micrographs of the same stage 16 embryo at different focal depths (A–C) stained with the anti-NRX antibody.

(A) Staining in ectodermal cells and tracheae, (B) salivary glands (anterior) and midline glia cells of the CNS, (C) pharynx, esophagus, proventriculus, salivary glands, and hindgut, but not Malpighian tubules.

(D) Three abdominal segments labeled with anti-NRX (green) and anti-Crumbs (red). Note the strong labeling in processes of midline glia (arrow) and glia-wrapping axons of the PNS (arrowhead).

(E) Hindgut labeled with anti-Crumbs (red, apical) and anti-NRX (green, apicolateral). There is no overlap between the two markers: NRX is localized apicolaterally where SJs occur; Crumbs is apically restricted.

(F) Hindgut double labeled with anti-NRX (green) and anti-D4.1/CORACLE (red). The double arrow shows the length of a single gut cell: (a) = apical and (b) = basal. NRX (green) and D4.1-CORACLE (red) fully colocalize. This is observed in almost all embryonic cells and optical sections studied.

a homophilic cell adhesion molecule in this cell adhesion assay, and it does not cause aggregation in the presence of many proteins that have been expressed in S2 cells such as Gliotactin (Auld et al., 1995). Obviously, NRX may be a heterophilic cell adhesion molecule whose ligand remains to be identified.

### Mutations in *nrx* Cause Embryonic Lethality

To determine *nrx* function in vivo, we initiated a genetic analysis. Three chromosomal deficiences uncover 68F at least partially (Figure 4A). Southern analysis of genomic DNA showed that the genomic Nrx-1 phage is uncovered by *Df(3L)BK9* and *Df(3L)vin*$^{8}$, placing *nrx* at 68F3–6. To obtain *nrx* mutations, *ru h st ry e* flies were mutagenized with ethyl methanesulfonate, and lethal mutations that failed to complement *Df(3L)vin*$^{5}$ (68A2–3;69A1–3) were isolated. In addition, previously isolated mutations mapping to this interval were mapped by complementation (Figure 4A). To demonstrate that *l(3)68Ff* corresponds to *nrx*, the genomic insert of the Nrx-1 phage (Figure 1A) was cloned into a transformation vector, and six independent transformant strains (*P{nrx*$^{+}$*}* 6*a*, 7*c*, 7*h*, 7*e*, 4*a*, and 7*f*) were obtained and analyzed for their ability to rescue *nrx* mutations. All transformant chromosomes fully rescued the embryonic lethality of all *l(3)68Ff* alleles in trans to *Df(3L)BK9*. These data demonstrate that mutations in complementation group *l(3)68Ff* are mutations in *nrx*.

No allele produces adult survivors in trans with *Df(3L)BK9* and *Df(3L)vin*$^{8}$, and most alleles are embryonic lethal in trans with *Df(3L)BK9* (Figure 4B). Heteroallelic mutant adults (escapers) were occasionally obtained (Figure 4B). Adult escapers that carry transheterozygous combinations of *nrx*$^{14,\ 319,\ 575,\ 711,\ 2511}$ were obtained, suggesting that these mutations represent hypomorphic alleles (Figure 4B). Various structures are affected in *nrx* mutant escapers: eyes are rough, wings exhibit notching and vein broadening, and legs exhibit duplications and malformations. In addition, antibody stainings of third-instar larvae reveal that imaginal disks express NRX at SJs (data not shown). Other alleles, *nrx*$^{4304,\ 4865,\ 4164,\ 4025,\ 46}$, are strong hypomorphic alleles or null alleles, as they are embryonic lethal in trans to deficiencies and to each other.

### Nervous System Function Is Impaired in *nrx* Mutations

The most striking behavioral defect in *nrx* embryos is a severe reduction of coordinated muscle propagation waves. In addition, tracheae do not fill with air in mutants. The *nrx*$^{4304,\ 46}$*/Df(3L)BK9* embryos seemed to be the most severely affected, showing a complete absence of muscle-propagation waves. These movement defects are similar to those observed in other mutants in which neurotransmitter release is abolished (Broadie et al., 1995; Schulze et al., 1995).

To determine how *nrx* mutations block neuromuscular communication, we systematically analyzed nervous system development and function in mutant embryos. When *nrx*$^{4304}$*/Df(3L)BK9* and *Df(3L)BK9/Df(3L)vin*$^{8}$ mutant embryos are stained with neuronal-specific markers, axons are seen to cross segmental boundaries in 10%–20% of mutant embryos (data not shown, see below). Hence, there is no absolute requirement for NRX in axonal pathfinding, but its absence results in a higher propensity for neuronal connectivity defects. In addition, antibody stainings reveal that chordotonal scolopales acquire an abnormal rounded shape in *nrx* embryos (Figure 5Bc), compared to the specific fusiform shape in wild-type embryos (Figures 5Ba and 5Bb). NRX is localized to the subcellular area where scolopale SJs have been reported to form (Figure 5Ba) (S. D. Carlson et al., submitted). These defects suggest that lack of NRX affects the SJs between scolopale and cap cells, resulting in abnormal morphology of scolopales.

Taken together, these morphological defects are unlikely to account for the severe behavioral defects that we observe. Even if target recognition occurs properly,

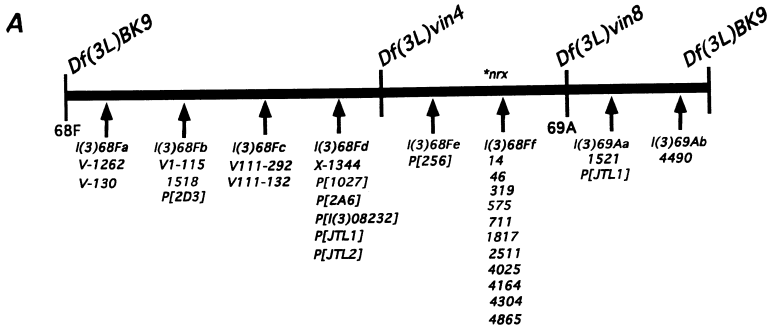


B

| | 14 | 46 | 319 | 575 | 711 | 1817 | 2511 | 4025 | 4164 | 4304 | 4865 |
|---|---|---|---|---|---|---|---|---|---|---|---|
| 14 | +/- | | | | | | | | | | |
| 46 | - | - | | | | | | | | | |
| 319 | - | - | - | | | | | | | | |
| 575 | - | - | +/- | - | | | | | | | |
| 711 | - | - | + | - | +/- | | | | | | |
| 1817 | - | - | - | - | - | | | | | | |
| 2511 | +/- | - | + | + | + | - | - | | | | |
| 4025 | - | - | - | - | - | - | - | - | | | |
| 4164 | - | - | - | - | - | - | - | - | - | | |
| 4304 | - | - | - | - | - | - | - | - | - | - | |
| 4865 | - | - | - | - | - | - | - | - | - | - | - |
| Df(3L)vin4 | + | + | + | + | + | + | + | + | + | + | + |
| Df(3L)vin8 | - | - | - | - | - | - | - | - | - | - | - |
| Df(3L)BK9 | - | - | - | - | - | - | - | - | - | - | - |
| %Embryonic Lethality with Df(3L)BK9 | 27 | 27 | 8 | 29 | 14 | 23 | 28 | 26 | 27 | 27 | 28 |

- = no adult progeny
+ = > 1% expected progeny
+/- = < 1% expected progeny

Figure 4. Isolation and Complementation Data of *nrx* Mutants

(A) We obtained six P-elements from FlyBase (1994) and some ethyl methanesulfonate alleles from H. Benes. Local hopping with PBGT-V036 allowed recovery of P[JTL1] and P[JTL2]. However, all *nrx* alleles were isolated using ethyl methanesulfonate. All mutations can be at least partially rescued by the Nrx-1 genomic clone (1B) in trans to *Df(3L)BK9* in transgenic animals. The complementation groups are not ordered.

(B) Complementation data and lethality of *nrx* mutants. All *nrx* mutations are lethal over *Df(3L)BK9* and *Df(3L)vin8*. The embryonic lethality is shown at the bottom (25% = lethal).

and neuromuscular contacts are established, differentiation of the neuromuscular junction (NMJ) can still fail (Prokop et al., 1996). Hence, we investigated the morphology of NMJs using transmission electron microscopy (TEM). Normal neuromuscular synapses are characterized by presynaptic active zones, with a T-shaped density and clustered vesicles (Seecof et al., 1972). Analyses of $nrx^{46,\ 4025,\ 4304}$ mutant embryos did not reveal morphological synaptic defects (Figure 6A) and indicate that docking of synaptic vesicles at active zones is not affected in the synapses examined at this level of resolution.

We next carried out electrophysiological studies at the embryonic NMJ. About 10% of the NMJs examined failed to respond to nerve stimulation (Figure 6B), indicating that a fraction of synapses fail to form in *nrx* mutants, in agreement with the growth cone guidance defects observed in some mutant embryos. In the other 90% of NMJs examined, the mean amplitude of evoked synaptic transmission is reduced by 40%–45% in mutant embryos ($nrx^{4304/4304}$; $nrx^{4304}$/*Df*; $nrx^{46/46}$; $nrx^{46}$/*Df*), compared to wild-type embryos (Figure 6B). Iontophoresis of L-glutamate (the excitatory neurotransmitter) onto mutant NMJs resulted in essentially wild-type responses (Figure 6B), indicating that the postsynaptic receptor field develops normally. Thus, NRX function appears to be required presynaptically to facilitate transmission.

The 40%–45% decrease in evoked response described above cannot account for the total paralysis observed in the *nrx* mutant embryos, as mutants with <10% of wild-type neurotransmitter release still display some muscle contractions (Littleton et al., 1993; Broadie et al., 1994). Therefore, we surmised that other defects must compound the reduction in evoked response. As shown in Figure 6C, wild-type NMJs exhibit robust periodic bursts of endogenous transmission. These bursts of activity correlate with muscle contractions that permit first-instar larvae to hatch from the egg case (Broadie and Bate, 1993). In *nrx* mutant embryos ($nrx^{4304}$/$nrx^{4304}$ and $nrx^{4304}$/*Df(3L)BK9*), these bursts are reduced, suggesting a suppression of endogenous activity in motoneurons. Interestingly, some muscle contractions are observed in *nrx* mutants upon dissection of embryos in low [$K^+$] saline recording solutions (2 mM). These saline solutions are much lower in potassium concentration than hemolymph, which is approximately 40 mM $K^+$ (Auld et al., 1995). Therefore, we recorded in 40 mM extracellular $K^+$ in mutant and wild-type embryos. As shown in Figure 5C, wild-type embryos still show robust excitatory junctional currents (EJCs) when muscles are voltage-clamped at −60 mV in 2 mM and 40 mM $K^+$. However, mutant embryos recorded at 40 mM $K^+$ show a severe depression of spontaneous synaptic activity, compared to wild-type embryos. At 40 mM extracellular [$K^+$], some activity remains, but the EJC bursts required for coordinated muscle contractions are essentially absent. A similar defect occurs in *gliotactin* mutant embryos in which the blood-nerve barrier is broken down. Thus, *nrx* mutant embryos exhibit a reduced ability to propagate action potentials in high [$K^+$], similar to that observed in *gliotactin* mutants (Auld et al., 1995). This conclusion is corroborated by the observation that complete paralysis of *nrx* mutant embryos is partially reverted when the embryos are dissected in 2 mM $K^+$. Although it is unknown how changes in [$K^+$] affect glial permeability, the ability of wild-type glia to support action potential propagation at different [$K^+$] argues against other contributing glial defects. Therefore, we

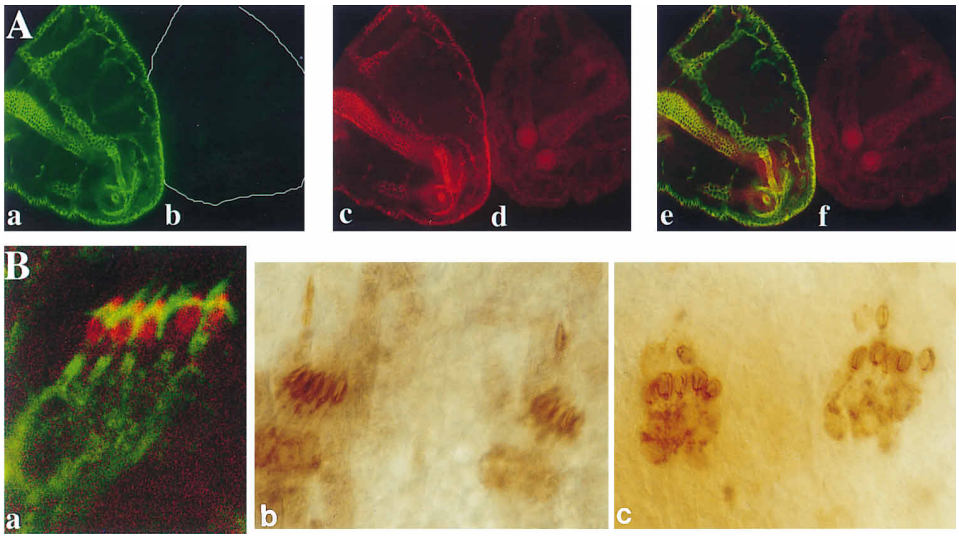


Figure 5. Mislocalization of D4.1-Coracle and Defective Chordotonal SJs in *nrx* Mutants

(A) Confocal microscopic analysis of the localization of NRX and D4.1-Coracle in *nrx* mutants.

(Aa/Ab) Posterior end of a wild-type embryo and mutant embryo (white outline) labeled with NRX. NRX is absent in $nrx^{4304}$ mutants.

(Ac/Ad) The same embryos labeled with anti-D4.1/Coracle antibody. Note the faint staining and diffuse localization of the D4.1-Coracle protein in the *nrx* mutant compared to the wild type.

(Ae/Af) Overlay of (Aa/Ab) and (Ac/Ad) shows the colocalization of both proteins to SJs in the wild-type embryo.

(Ba) The five lateral chordotonal neurons stained with anti-NRX (green) and anti-Crumbs (red). Crumbs labels the scolopales. NRX labels the SJs between the cap and sheath cells, surrounding and capping the scolopales. NRX also surrounds the dendrite.

(Bb) Two clusters of wild-type lateral chordotonal neurons stained with MAb 21A6. Note the fusiform shape of the scolopales at the tip of the dendrites.

(Bc) *nrx* mutant lateral chordotonal scolopales are round instead of fusiform, and the arrays are disorganized.

conclude that NRX expression in glial SJs is required for proper axonal insulation and blood–nerve barrier formation.

### *nrx* Mutations Disrupt the Formation of pSJs

To test how SJs might be affected in *nrx* mutant embryos, we analyzed $nrx^{4304}$ for expression of two proteins known to be localized to SJs in Drosophila: DLG and D4.1-Coracle. *nrx* mutant embryos were double labeled with anti-NRX and anti-DLG or anti-D4.1/Coracle. We observed no obvious defects in the localization of the DLG protein (data not shown). However, in *nrx* mutant embryos, D4.1-Coracle is not restricted to SJs (compare Figures 5Ad and 5Ac). These results suggest that the short cytoplasmic portion of NRX that shows homology to glycophorin C is required to localize D4.1-Coracle to SJs, creating a parallel with red blood cell cytoskeletal anchoring proteins. *coracle* mutants have been shown to display a cell-migration defect affecting dorsal closure (Fehon et al., 1994). Severe *nrx* alleles also cause a defect in dorsal closure, resulting in a small dorsal hole, consistent with abnormal function of D4.1-Coracle in *nrx* embryos (data not shown). Hence, SJs may play a role in targeting cytoskeletal components and contribute to intercellular communication and cell migration during dorsal closure.

These findings suggest that pSJs are impaired in the absence of *nrx*. To test this hypothesis further, we investigated the ultrastructural morphology of pSJs in *nrx* mutant embryos using TEM. In wild-type embryos, pSJs were identified in epidermis, trachea, perineurium, and glial sheaths of nerves, with the membranes of the two attached cells separated by a 15 nm intercellular cleft. This cleft is traversed by electron-opaque septa that are separated by 15 nm and form the typical ladder-like appearance of pSJs (Figure 7A). When sectioned obliquely, the cleft of pSJs reveals a characteristic honeycomb-like pattern formed by regular arrays of septae (Figure 7B). A further type of SJ, the sSJs, are located in the midgut and amnioserosa (Lane and Skaer, 1980; Tepass and Hartenstein, 1994) and are characterized by evenly spaced electron-dense membranes, comparable to pSJs. In contrast to pSJs, sSJs rarely contain transverse septae, and their intercellular cleft is filled with an unstructured electron-dense matter.

In *nrx* mutant embryos, sSJs appear unaffected. However, in *nrx* embryos ($nrx^{4304,\ 4025,\ 46}$/*Df(3L)BK9*), using five different fixation procedures, the typical ladder-like septae of pSJs were absent in ectodermal cells and perineural glia-ensheathing peripheral axons (Figures 7D and 7E). Apposing membranes in these tissues have a smooth and electron-dense appearance, and unstructured cleft material is apparent. When sectioned obliquely, the honeycomb pattern imparted by the transverse septae is absent, and features of sSJs are seen (compare Figures 7B and 7F). Thus, pSJs in *nrx* mutant embryos lose their characteristic ladder-like septae that distinguish them from sSJs.

To investigate this phenotype in more detail, specimens were negatively stained by perfusion with colloidal lanthanum. Upon lanthanum treatment, obliquely sectioned midgut sSJs in wild-type and *nrx* mutant embryos

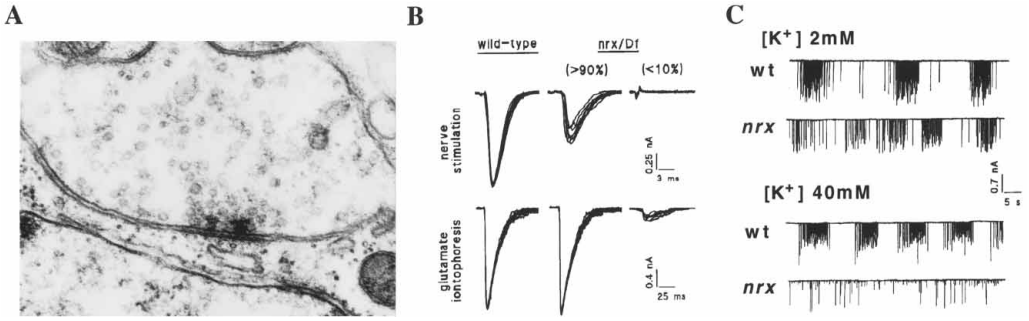


Figure 6. NRX is Required for Glial Function and Formation of the Blood-Nerve Barrier

(A) TEM micrograph of a NMJ of a *nrx* mutant embryo exhibits normal morphological characteristics: a presynaptic T-bar with clustered vesicles, smooth, electron-dense pre- and postsynaptic membranes, and regularly structured cleft material.

(B) Synaptic function at the mature embryonic NMJ assayed by suction-electrode stimulation of the motor nerve (presynaptic function) and glutamate iontophoresis onto the muscle-receptor field (postsynaptic function) and measured by recording the resultant synaptic current in the voltage-clamped (−60 mV) muscle. Each trace shows 10 superimposed trials recorded at 1 Hz stimulation frequency. In wild-type embryos, nerve stimulation and glutamate iontophoresis result in robust, high fidelity synaptic transmission. In $nrx^{4304}/nrx^{4304}$ and $nrx^{4304}/Df$ embryos, two distinct classes are observed. The majority of synapses (>90%) show significantly decreased synaptic transmission but normal glutamate response, indicating a presynaptic transmission defect. A small number of synapses (<10%) show no synaptic transmission and a weak postsynaptic glutamate response, consistent with a failure in neuronal pathfinding or synaptogenesis. The reductions of evoked transmission are only enhanced 5% when homozygous $nrx^{4304,46}$ embryos are compared to $nrx^{4304,46}/Df(3L)BK9$ embryos, indicating that both alleles correspond to severe loss of function mutations. Embryos that lack *nrx* (*Df(3L)BK9/Df(3L)BK9*) showed similar defects.

(C) Endogenous synaptic transmission at the mature embryonic NMJ occurs as bursts of EJCs underlying the periodic body-muscle contractions during locomotion. In wild-type embryos, robust EJC bursts are recorded at 2 mM external $K^+$ (standard recording condition) and 40 mM external $K^+$ (estimated physiological $K^+$ level). In $nrx^{4304}/nrx^{4304}$ and $nrx^{4304}/Df$ embryos, EJC bursts are recorded at 2 mM external $K^+$, though the amplitude and frequency of EJCs are significantly decreased. However, at physiological $K^+$ concentrations (40 mM), EJC bursts are eliminated, and the residual transmission is present as a low frequency of largely unpatterned EJCs. This $K^+$-dependent transmission defect is consistent with a glial function for NRX and explains the paralytic phenotype.

showed no obvious defects (data not shown). In addition, pSJs in *nrx* mutant embryos showed some normal features, such as rows of ring-shaped structures, common to all pSJs and sSJs (data not shown). However, in contrast to sSJs, pSJs in *nrx* mutant embryos are clearly affected, with the regularly spaced septae absent in most ectodermal tissues of 11 analyzed specimens (compare Figures 7C and 7G). These septae are specific to pSJs and are thinner and more regularly arranged than those in sSJs (Lane and Skaer, 1980). Thus, positive- and negative-stained transmission micrographs reveal pSJs, but not sSJs, to be affected in *nrx* mutant embryos. The affected pSJs retain some characteristics of SJs but lack the regularly arranged septae, the princi-

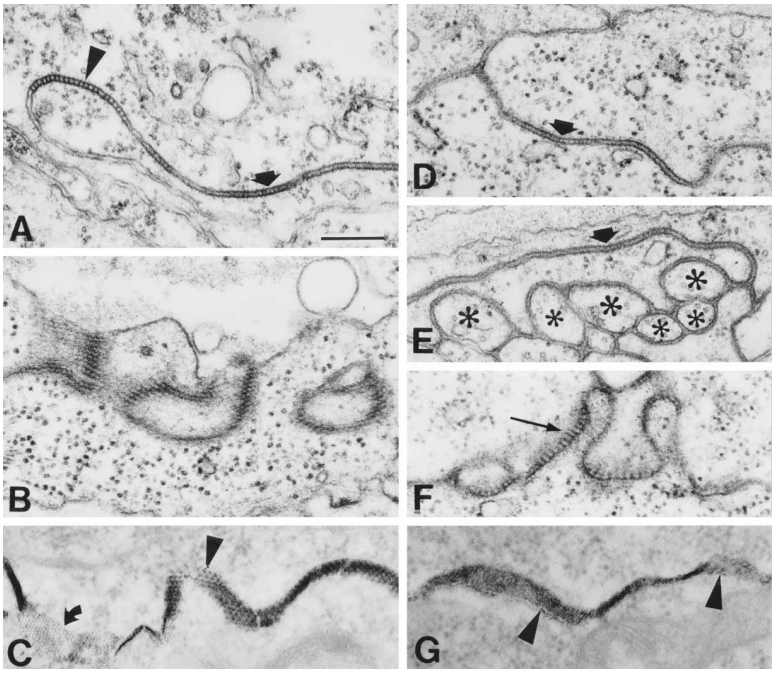


Figure 7. TEM Reveals Lack of Septae in PSJs of *nrx* Mutant Embryos

SJs in (A–C) ectoderm of wild-type embryos and in (D, F, and G) ectoderm and (E) glial SJs of *nrx* mutant embryos. Stretches of closely apposed electron-dense membrane with unstructured cleft material can be found in all SJs (short arrows).

(A) Septae are prominent and regularly spaced in ectodermal pSJs of wild type (arrowhead) but are absent ([D] and [E]) in ectodermal and glial SJs of *nrx* mutant embryos (asterisks indicate axonal profiles).

(B) Obliquely sectioned SJs appear as honeycomb-like structures in ectodermal pSJs of wild type and as regularly spaced parallel lines in the (F) ectoderm of mutant embryos (normally seen in smooth SJs).

(C and G) Infiltration with lanthanum reveals septae, which are densely packed in ectodermal pSJs of wild type (arrowhead in [C]; the bent arrow in [C] points at a gap junction) but are (G) rare and structurally affected in ectodermal SJs of *nrx* embryos. Septa of pSJs are thinner and more regularly and densely arranged than septa in sSJs. The scale bar = 200 μm.

ple feature distinguishing pSJs from sSJs. These results show that NRX is an integral component of pSJs and is either part of the transverse septae or required for their formation.

## Discussion

### NRX Is a Novel Marker for pSJs

We have isolated a new member of the neurexin family, *neurexin IV*. NRX has the conserved modular arrangement of the domains of neurexins I–III (Ushkaryov et al., 1992; Ushkaryov and Sudhof, 1993) but exhibits a different amino-terminal domain, in which a DS domain replaces a laminin G domain and an EGF-like repeat. The DS domain was originally found in the discoidin proteins of Dictyostelium and appears to bind carbohydrates (Ito et al., 1994). The overall domain structure of Drosophila NRX appears to be conserved in vertebrates, and a homologous human gene is expressed in neuronal and nonneuronal embryonic tissues, unlike other vertebrate neurexins.

NRX is localized to pSJs and is the first marker to identify these junctions specifically at all stages and in all cells documented to contain pSJs. Multiple lines of evidence suggest that NRX is essential for pSJ formation and function. First, NRX is expressed in all tissues known to have pSJs and appears about 1 hr prior to their appearance. NRX is not expressed in tissues devoid of pSJs, where zonula adherens or sSJs have been documented. Second, the protein is localized to peripheral and subperineural glial junctions, which are known to contain pSJs and have been proposed to form the Drosophila blood–nerve–brain barrier. Third, the protein does not colocalize with Crumbs, an apical marker that delimits the zonula adherens (Wodarz et al., 1995). Fourth, NRX colocalizes with Fasciclin III, an SJ marker in salivary glands, and D4.1-Coracle, which labels all known pSJs except those of the nervous system. Fifth, mutants that lack NRX are paralyzed due to a breakdown of the blood–nerve barrier, indicating a functional defect in SJs. Sixth, loss-of-function *nrx* alleles cause a mislocalization of D4.1-Coracle in tissues where they are coexpressed, and *nrx* mutants show a similar phenotype to loss of function *coracle* alleles. Finally, TEM analysis demonstrates that the typical ladder-like septa that define pSJs are absent in *nrx* mutants.

### *nrx* Mutant Embryos Reveal Novel Functions for SJs

Based on our observations, we can begin to describe specific functions that pSJs are likely to play during development. First, pSJs are found in ectodermal epithelia that are in contact with the environment and in glia that ensheath the nervous system. It is likely that these cells protect the embryo and the nervous system by serving as a selective-diffusion barrier. In vertebrates, tight junctions have been proposed to serve this role. However, such junctions are virtually absent in insects, and it has been proposed that pSJs might serve this barrier function instead. Each SJ may confer partial impermeability, so that together they form a barrier that protects neurons from high potassium concentration in the hemolymph of insects (Hoyle, 1952; Juang and Carlson, 1992). The phenotype of *nrx* mutants indicates that the septae of pSJs are required to form the blood–brain–nerve barrier in vivo, providing further evidence that tight junctions in vertebrates and SJs in insects are functionally similar (Willott et al., 1993). At the electrophysiological level, the blood–nerve barrier defect is similar to that observed in embryos mutant for *gliotactin*, a gene expressed in glial cells and required to insulate motoneurons (Auld et al., 1995). Gliotactin shows 29% identity and 50% similarity to vertebrate neuroligin-I, which has been shown to be the ligand of certain vertebrate neurexins (Ichtchenko et al., 1995). However, given the failure of S2 cells, which express Gliotactin and NRX to aggregate, it remains to be determined if these two proteins interact directly in Drosophila.

Two other defects were also revealed in the electrophysiological studies: a decrease in evoked neurotransmitter release, compared to wild-type embryos, and occasional failure to form synapses. The first defect could be due to a docking defect of synaptic vesicles or to a reduced activation of vesicle fusion upon $Ca^{2+}$ influx. However, Drosophila NRX does not localize to synapses, and we therefore surmise that this defect is likely secondary to glial dysfunction. Second, <10% of the synapses fail to form, suggesting defects in neuronal pathfinding or synapse formation. Glial cells have been implicated in growth cone guidance, and the misrouting defects observed in *nrx* mutant embryos strengthen this hypothesis. Finally, the defects observed in the scolopales of chordotonal neurons and localization of NRX to SJs of cap and sheath cells surrounding the scolopales suggest that this recently described peripheral blood–nerve barrier (S. D. Carlson et al., submitted) is also disrupted in *nrx* mutants.

A second major function of SJs is to provide a mechanical link between cells, being in part responsible for the densely packed arrangement of epithelial sheaths. This function is obviously affected in *dlg* mutants, causing a breakdown of epithelial sheaths and subsequent overgrowth (Woods and Bryant, 1991). In contrast, tissues remain intact, and DLG still localizes to sites of membrane contact in *nrx* mutant embryos. Our TEM analysis demonstrates that *nrx* mutations do not affect characteristics of SJs that are shared by pSJs and sSJs, such as the evenly spaced extracellular cleft and the electron-dense appearance of the membranes. Therefore, it is unlikely that NRX functions in the adhesive properties required to connect the two apposing membranes, consistent with the lack of aggregation in S2 cells expressing NRX. Instead, NRX is likely to form or anchor the ladder-like septae characteristic of pSJs.

Finally, pSJs have been suggested to be involved in cell signaling. The data suggest a role for neurexins in addition to barrier formation. The requirement of NRX for proper localization of the Drosophila homolog of protein 4.1, Coracle, an SJ-associated protein, shows that NRX forms a link between the extracellular environment and intracellular components of SJs. This link has important functional implications, as it affects dorsal closure and cell migration late in embryonic development. It is interesting to note that human dlg protein binds to protein 4.1 (Lue et al., 1994), and that glycophorin C, protein 4.1, and p55, a guanylate kinase domain

containing protein, have been shown to form a complex in vertebrates (Marfatia et al., 1994). The function of this complex has not been precisely defined. The CASK protein, another guanylate kinase domain containing protein, has been shown to bind previously identified vertebrate neurexins and to be expressed in nonneuronal tissues (Hata et al., 1996). Hence, three proteins with PDZ, guanylate kinase, and SH3 domains (p55, DLG, and CASK) are associated with SJs or interact with neurexins and have been proposed to be involved in inter- and intracellular signaling. Defects in these signaling pathways may underlie the dorsal closure defects in *nrx* mutants. We are presently focusing on characterizing the severe defects in adult structures observed in partial loss of function *nrx* alleles that further implicate NRX and SJs in imaginal development and cellular communication.

## Experimental Procedures

### Fly Stocks and Mutagenesis

The *vin* deficiencies are described by Hoogwerf et al. (1988). To obtain mutations in *nrx*, *ru h st ry e* males were treated with ethyl methanesulfonate (Lewis and Bacher, 1968). Approximately 10,000 mutagenized chromosomes were tested for lethality over *Df(3L)vin5* and *Df(3L)vin7*. Mutations that failed to complement *Df(3L)vin5* and *Df(3L)vin7* were tested over *Df(3L)BK9, Df(3L)vin4,* and *Df(3L)vin8.* As shown in Figure 4A, this allowed us to identify and map mutation *1518* to *l(3)68Fb*, as well as 11 mutations between the proximal break points of *Df(3L)vin4* and *Df(3L)vin8*. Mutations *1521* and *4490* identify two complementation groups to the right of *nrx*. Other mutations shown in Figure 4A are described in the legend.

### Isolation of Genomic and cDNA Clones

Degenerate polymerase chain reaction primers derived from the EGF-like repeats (forward primer coding for amino acids S, [G, A, S, R], [H, K], G, [L, N], C; reverse primer coding for amino acids C, [N, D], C, [R, E, H], [V, W], S) allowed amplification of a 1320 bp fragment harboring two laminin G domains flanked by two EGF-like repeats that showed homology to rat neurexins. This permitted isolation of cDNAs and genomic fragments.

### Generation of Antibodies and Immunohistochemical Staining

A peptide corresponding to the 15 aa from the C-terminal (1269–1283) was used to generate a polyclonal antiserum in rabbits. This serum was affinity purified and used at 1:500 dilution.

### Electrophysiology

The electrophysiological recordings were carried out as described in Broadie and Bate, 1993, Broadie et al., 1995, and Auld et al., 1995. All records were made from muscle 6 in abdominal segment A2 in mature embryos (22–24 hr AEL).

### Electron Microscopy

Late stage 17 embryos were injected with 5% glutaraldehyde, followed by 1 hr postfixation in 2.5% glutaraldehyde (Prokop and Technau, 1993). Preparations were washed, fixed for 1 hr in 1% osmium in $dH_2O$, washed, and treated en bloc with an aqueous 2% solution of uranyl acetate for 30 min. In lanthanum infiltration experiments, mature embryos were injected with 5% glutaraldehyde. For subsequent steps, solutions contained 2% lanthanum nitrate. The uranyl-acetate step was omitted. Specimens were dehydrated and transferred to Araldite. Serial sections of 30–50 nm thickness were obtained, postcontrasted with lead citrate for 5–10 min, and analyzed on a Jeol 200CX.

## Acknowledgments

We thank Doris Martin for technical assistance, Markus Noll for libraries, and Beth Ostermeyer for human nrx IV. We thank Richard Atkinson, Becky Scott, and Michael Macini for help with confocal microscopy. We thank Richard Atkinson, Kwang Choi, Kyung Cho, Karen Schulze, Mark Wu, and Artur Kania for suggestions. We thank Rick Fehon, Helen Benes, Todd Laverty, Kathy Matthews, and the Indiana Stock Center for fly strains. A. P. and K. B. thank Michael Bate, in whose laboratory their work was carried out, and A. P. thanks H. Skaer and N. J. Lane for discussions. This work was supported by an NIH training grant to J. T. L., an NIH grant (HD09948) to J. A. L, and an NIH grant to H. J. B. A. P. was funded by a Human Capital and Mobility Fellowship (European Union) and by a Fellowship from the Lloyd's of London Tercentenery Foundation. K. B. was a Research Fellow of Girton College, Cambridge, whose work was supported by the Wellcome Trust and an Alfred P. Sloan Fellowship. H. J. B. is an Associate Investigator of the Howard Hughes Medical Institute. Reprint requests should be sent to H. J. B.

Received April 21, 1996; Revised October 10, 1996.

## References

Auld, V.J., Fetter, R.D., Broadie, K., and Goodman, C.S. (1995). Gliotactin, a novel transmembrane protein on peripheral glia, is required to form the blood-nerve barrier in *Drosophila*. Cell *81*, 757–767.

Bieber, A.J. (1994). Analysis of cellular adhesion in cultured cells. In *Drosophila melanogaster*: Practical Uses in Cell and Molecular Biology, L.S.B. Goldstein and E.A. Fyrberg, eds. (San Diego, California: Academic Press), pp. 683–713.

Bock, G., and Clark, S. (1987). Junctional Complexes of Epithelial Cells (New York: John Wiley & Sons).

Broadie, K.S., and Bate, M. (1993). Development of the embryonic neuromuscular synapse of *Drosophila melanogaster.* J. Neurosci. *13*, 144–166.

Broadie, K., Bellen, H.J., DiAntonio, A., Littleton, J.T., and Schwarz, T.L. (1994). The absence of synaptotagmin disrupts excitation-secretion coupling during synaptic transmission. Proc. Natl. Acad. Sci. USA *91*, 10727–10731.

Broadie, K., Prokop, A., Bellen, H.J., O'Kane, C.J., Schulze, K.L., and Sweeney, S.T. (1995). Syntaxin and synaptobrevin function downstream of vesicle docking in *Drosophila*. Neuron *15*, 663–673.

Brody, L.C., Abel, K.J., Castilla, L.H., Couch, F.J., McKinley, D.R., Yin G., Ho, P., Merajver, S., Chandrasekharappa, S.C., Xu, J., et al. (1995). Construction of a transcription map surrounding the *BRCA1* locus of human chromosome 17. Genomics *25*, 238–247.

Brown, N.H., and Kafatos, F.C. (1988). Functional cDNA libraries from *Drosophila* embryos. J. Mol. Biol. *203*, 425–437.

Cho, K.-O., Hunt, C.A., and Kennedy, M.B. (1992). The rat brain postsynaptic density fraction contains a homolog of the Drosophila discs-large tumor suppressor protein. Neuron *9*, 929–942.

Fehon, R.G., Dawson, I.A., and Artravanis-Tsakonas, S. (1994). A *Drosophila* homologue of membrane-skeleton protein 4.1 is associated with septate junctions and is encoded by the *coracle* gene. Development *120*, 545–557.

FlyBase (1994). The *Drosophila* genetic database. Nucleic Acids Res., *22*, 3456–3458.

Friedman, L.S., Ostermeyer, E.A., Lynch, E.D., Welsch, P., Szabo, C. I., Meza, J.E., Anderson, L.A., Dowd, P., Lee, M.K., Rowell, S.E., et al. (1995). 22 genes from chromosome $17_q21$: cloning, sequencing, and characterization of mutations in breast cancer families and tumors. Genomics *25*, 256–263.

Fristrom, D.K. (1982). Septate junctions in imaginal disks of *Drosophila*: a model for the redistribution of septa during cell rearrangement. J. Cell Biol. *94*, 77–87.

Grawe, F., Wodarz, A., Lee, B., Knust, E., and Skaer, H. (1996). The *Drosophila* genes *crumbs* and *stardust* are involved in the biogenesis of adherens junctions. Development *122*, 951–959.

Hata, Y., Butz, S., and Sudhof, T.C. (1996). Cask: a novel *dlg/PSD95* homologue with an n-terminal calmodulin-dependent protein kinase domain identified by interaction with Neurexins. J. Neurosci. *16*, 2488–2494.

Hoogwerf, A.M., Akam, M., and Roberts, D. (1988). A genetic analysis

of the *rose-gespleten* region (68C8–69B5) of *Drosophila melanogaster*. Genetics *118*, 665–670.

Hoyle, G. (1952). High blood potassium in insects in relation to nerve conduction. Nature *169*, 281–282.

Ichtchenko, K., Hata, Y., Nguyen, T., Ullrich, B., Missler, M., Moomaw, C., and Sudhof, T.C. (1995). Neuroligin 1: a splice site-specific ligand for B-Neurexins. Cell *81*, 435–443.

Ito, N., Phillips, S.E.V., Yadav, K.D.S., and Knowles, P.F. (1994). Crystal structure of a free radical enzyme, galactose oxidase. J. Mol. Biol. *238*, 794–814.

Itoh, M.S., Nagafuchi, S., Yonemura, R., Kitani-Yasuda, T., and Tsukita, S. (1993). The 220 kDa protein colocalizing with cadherins in non-epithelial cells is identical to Z0–1, a tight junction-associated protein in epithelial cells: cDNA cloning and immunoelectron microscopy. J. Cell Biol. *121*, 491–502.

Jesaitis, L.A., and Goodenough, D.A. (1994). Molecular characterization and tissue distribution of Z0–2, a tight junction protein homologous to Z0–1 and the Drosophila discs-large tumor supressor protein. J. Cell Biol. *124*, 949–961.

Juang, J.-L., and Carlson, S.D. (1992). A blood-brain barrier without tight junctions in the fly central nervous system in the early postembryonic stage. Cell Tissue Res. *270*, 95–103.

Kirkpatrick, C., and Peifer, M. (1995). Not just glue: cell-cell junctions as cellular signalling centers. Curr. Opin. Genet. Dev. *5*, 56–65.

Lahey, T., Gorczyca, M., Jia, X.-X., and Budnik, V. (1994). The Drosophila tumor suppressor gene *dlg* is required for normal synaptic bouton structure. Neuron *13*, 823–835.

Lane, N.J. (1991). Cytoskeletal associations with intercellular junctions in arthropods. In Form and Function in Zoology, G. Lanzavecchi and R. Valvassori, eds. (Munich: Modena), pp. 87–102.

Lane, N.J., and Skaer, H.B. (1980). Intercellular junctions in insect tissues. In Advances in Insect Physiology, M.J. Berridge, J.E. Treherne, and V.B. Wigglesworth, eds. (London: Academic Press), pp. 35–213.

Lane, N.J., Skaer, H.I., and Swales, L.S. (1977). Intercellular junctions in the central nervous system of insects. J. Cell Sci. *26*, 175–199.

Lewis, E.B., and Bacher, F. (1968). Mutagenesis with ethyl methanesulfonate. Drosoph. Inf. Serv. *43*, 193.

Littleton, J.T., Stern, M., Schulze, K., Perin, M., and Bellen, H.J. (1993). Mutational analysis of *Drosophila synaptotagmin* demonstrates its essential role in $Ca^{2+}$-activated neurotransmitter release. Cell *74*, 1125–1134.

Locke, M. (1965). The structure of septate desmosomes. J. Cell Biol. *25*, 166–168.

Lue, R.A., Marfatia, S.M., Branton, D., and Chishti, A.H. (1994). Cloning and characterization of hdlg: the human homologue of the Drosophila disc large tumor suppressor binds to protein 4.1. Proc. Natl. Acad. USA *91*, 9818–9822.

Lux, S.E., and Palek, J. (1995). Disorders of the red cell membrane. In Blood Principles and Practice of Hematology, R.I. Handin, S.E. Lux, and T.P. Stossel, eds. (Philadelphia: J.B. Lippincott Company).

Marfatia, S.M., Lue, R.A., Branton, D., and Chishti, A.H. (1994). In vitro binding studies suggest a membrane-associated complex between erythroid p55, protein 4.1, and glycophorin C. J. Biol. Chem. *269*, 8631–8634.

Petrenko, A.G., Perin, M.S., Bazbek, A., Davletov, B.A., Ushkaryov, Y.A., Geppert, M., and Sudhof, T.C. (1991). Binding of synaptotagmin to the $\alpha$-latrotoxin receptor implicates both in synaptic vesicle exocytosis. Nature *353*, 65–68.

Prokop, A., and Technau, G.M. (1993). Cell transplantation. In Cellular Interaction in Development: A Practical Approach, D. Hartley, ed. (London: Oxford University Press), pp. 33–57.

Prokop, A., Landgraf, M., Rushton, E., Broadie, K., and Bate, M. (1996). Presynaptic development at the *Drosophila* neuromuscular junction: assembly and localization of presynaptic active zones. Neuron, *17* 617-626.

Schulze, K., Broadie, K., Perin, M., and Bellen, H.J. (1995). Genetic and electrophysiological studies of *Drosophila* syntaxin-1A demonstrate its role in nonneuronal secretion and neurotransmission. Cell *80*, 311–320.

Seecof, R.L., Teplitz, R.L., Gerson, I., Ikeda, K., and Donady, J.J. (1972). Differentiation of neuromuscular junctions in cultures of embryonic Drosophila cells. Proc. Natl. Acad. Sci. USA *69*, 566–570.

Tepass, U., and Hartenstein, V. (1994). The development of cellular junctions in the *Drosophila* embryo. Dev. Biol. *161*, 563–596.

Tsukita, S., Itoh, M., Nagafuchi, A., Yonemura, S., and Tsukita, S. (1993). Submembranous junctional plaques proteins include potential tumor suppressor molecules. J. Cell Biol. *123*, 1049–1053.

Ullrich, B., Ushkaryov, Y.A., and Südhof, T.C. (1995). Cartography of neurexins: more than 1000 isoforms generated by alternative splicing and expressed in distinct subsets of neurons. Neuron *14*, 497–507.

Ushkaryov, Y.A., and Südhof, T.C. (1993). Neurexin IIIa: extensive alternative splicing generates membrane-bound and soluble forms. Proc. Natl. Acad. Sci. USA *90*, 6410–6414.

Ushkaryov, Y.A., Petrenko, A.G., Geppert, M., and Südhof, T.C. (1992). Neurexins: synaptic cell surface proteins related to the $\alpha$-latrotoxin receptor and laminin. Science *257*, 50–56.

Willott, E., Balda, M.S., Fanning, A.S., Jameson, B., VanItallie, C., and Anderson, J.M. (1993). The tight junction protein Z0–1 is homologous to the *Drosophila* discs large tumor suppressor protein of septate junctions. Proc. Natl. Acad. Sci. USA *90*, 7834–7838.

Wodarz, A., Hinz, U., Engelbert, M., and Knust, E. (1995). Expression of Crumbs confers apical character on plasma membrane domains of ectodermal epithelia of *Drosophila*. Cell *82*, 67–76.

Woods, D.F., and Bryant, P.J. (1991). The *discs-large* tumor suppressor gene of *Drosophila* encodes a guanylate kinase homolog localized at septate junctions. Cell *66*, 451–464.

Woods, D.F., and Bryant, P.J. (1993a). Apical junctions and cell signalling in epithelia. J. Cell Sci. Suppl. *17*, 171–181.

Woods, D.F., and Bryant, P.J. (1993b). ZO-1, DlgA and PSD-95SAP90: homologous proteins in tight, septate and synaptic cell junctions. Mech. Dev. *44*, 85–89.

**EMBL Accession Number**

The accession number for the *nrx* sequence is X86685. The accession numbers for the human expressed sequence tags in Figure 1B are T27170, U18000, U17905, Z42448, and U18017.